Archives of Mining Sciences **45**, 4 (2000) 443–462

JAN ZAWADA *

ROCK CRUSHING BY PUNCHES AT VARIOUS VELOCITIES OF LOAD APPLICATION

O KRUSZENIU SKAŁ STEMPLAMI PRZY RÓŻNYCH PRĘDKOŚCIACH OBCIĄŻANIA

The paper is the continuation of the analysis on crushing mechanics foundations presented by the author in his previous works. In the paper there is presented the experimental analysis of two domestic rocks crushing by flat punches at various load application velocities within the range of 0.005 – 1000 [mm/s].

The solution scheme based on limit state theory was shown. The studies results were discussed: mechanical characteristics, limit pressures and crushing energy corresponding to different load parameters. The cognitive and practical conclusions were formulated in the paper.

Key words: crushing mechanics, limit states, Coulomb condition, modified Coulomb condition, mechanical characteristics, limit pressures, crushing energy.

Jednym z ważniejszych procesów elementarnych modelujących proces kruszenia w maszynach jest ściskanie bloku stemplami płaskimi realizowane w warunkach zbliżonych do płaskiego odkształcenia (rys. 1a, b). Analiza tego procesu (i innych procesów modelowych przebiegających z małymi prędkościami), opierająca się na teorii stanów granicznych, została szczegółowo przeprowadzona w pracach autora (Zawada 1976, 1995).

Weryfikacja doświadczalna rozwiązań teoretycznych dla kilku skał krajowych wykazała przydatność tej teorii do określania obciążeń powodujących pękanie bloków skał i do przewidywania postaci pękania. Nie wiadomo jednak, czy istnieje możliwość stosowania uzyskanych rozwiązań do obliczania procesów, w których prędkości obciążania rosną, a więc rosną także siły bezwładności. W teorii stanów granicznych nie są znane efektywne metody rozwiązywania zagadnień dynamicznych, nawet dla wypadków płaskiej czy osiowo-symetrycznej deformacji. Jednym z głównych celów tej pracy była więc próba odpowiedzi na tę kwestię. Sformułowano również inne cele.

W teoretycznej części pracy przedstawiono szkic analizy zagadnienia kruszenia bloku dwoma współosiowymi stemplami płaskimi i jednym stemplem płaskim (gdy blok spoczywa

* INSTYTUT MASZYN ROBOCZYCH I CIĘŻKICH, POLITECHNIKA WARSZAWSKA, 02-524 WARSZAWA, UL. NARBUTTA 84

na sztywnej podstawie) (rys. 1). Przyjęto następujące założenia: 1. proces przebiega w płaskim stanie odkształcenia. 2. ośrodek skalny jest ciągły, jednorodny, izotropowy i nieważki, 3. modelem ośrodka jest model sztywno-plastyczny, 4. warunkiem stanu granicznego jest liniowy warunek Coulomba oraz bardziej realistycznie opisujący właściwości skał w strefie rozciągania zmodyfikowany warunek Coulomba, 5. prawem fizycznym jest prawo stowarzyszone z warunkiem stanu granicznego. Układ równań zawierający warunki równowagi i warunek stanu granicznego, tzw. układ równań statycznych, pozwala określić nieznany stan naprężenia (stan graniczny), a układ równań kinematycznych zawierający związki między tensorem prędkości odkształcania a gradientem funkcji stanu granicznego, spełniającej rolę potencjału, pozwala określić pole prędkości przemieszczania ośrodka. Układy równań statycznych i kinematycznych rozwiązujemy metodą charakterystyk quasi-liniowych cząstkowych równań różniczkowych (Zawada, 1995). Na rys. 3 i 4 pokazano rozwiązania jednego z wymienionych zagadnień, tj. obciążanie bloku spoczywającego na podstawie jednym stemplem płaskim. Rozwiązania obejmują siatki charakterystyk naprężeń i prędkości, i plany prędkości przemieszczania punktów ośrodka (hodografy) przy przyjęciu warunku Coulomba i warunku zmodyfikowanego.

Druga część pracy opisuje badania doświadczalne. Polegały one na obciążeniu próbek prostopadłościennych o wymiarach $h = 30$ mm, $2s = 50$ mm, $2g = 10$ mm wg schematu z rys. 1b. Objęły one dwa rodzaje skał krajowych: marmur (z okolic Stronia Śl.) i wapień (z okolic Kielc), których obwiednie stanu granicznego wyznaczono wcześniej. Szerokość $2a$ naciskających stempli wynosiła: 0,5; 1,0; 2,2; 4,0; 10 [mm]. Prędkość v_0 przemieszczania stempla osiągała wartości 0,005; 0,5; 5,0; $50\frac{\text{mm}}{\text{s}}$ — marmur, $v_0 = 0{,}005$; 0,5; 5,0; $100\frac{\text{mm}}{\text{s}}$ wapień. Doświadczenia przeprowadzono na maszynie wytrzymałościowej „Instron" (model 1251).

Najważniejsze wyniki doświadczeń przedstawiono w tablicach 1 i 2 i w postaci wykresów. Tablica 1 zawiera dane marmuru — wartości sił maksymalnych, jakie występują w procesie obciążania oraz wartości energii kruszenia, tabela 2 zawiera dane wapienia. Wykresy zaś przedstawiają: 1. przykłady charakterystyk mechanicznych, tzn. zależność siły obciążającej P od przesunięcia Δl stempla przy różnych szerokościach $2a$ stempla i różnych prędkościach v_0 (rys. 5 i 6), 2. naciski graniczne p w funkcji stosunku $\frac{h}{a}$ przy różnych prędkościach v_0 (rys. 7) 3. energię pękania E_K w funkcji $\frac{h}{a}$ przy różnych prędkościach v_0 (rys. 8), 4. energię pękania E_K w funkcji v_0 przy różnych wartościach $\frac{h}{a}$ (rys. 9).

Istotnym elementem pracy jest analiza wyników doświadczeń. Interesujących spostrzeżeń dostarcza analiza charakterystyk mechanicznych. I tak przy wzrastających prędkościach obciążania marmur zachowuje się tak jak większość skał, tzn. obserwujemy tu zjawisko wzrostu oporu tego ośrodka przy odkształcaniu. Znacznie trudniej interpretować charakterystyki wapienia, pojawia się tu bowiem dziwny efekt obniżania wartości siły granicznej przy największej prędkości obciążania v_0. Przebieg krzywych $P = f(\Delta l)$ przy różnych prędkościach v_0 odbiega również od przebiegu typowego dla skał. Naciski graniczne p, co przewiduje teoria stanów granicznych, rosną przy zwiększających się wartościach $\frac{h}{a}$, a więc są największe dla stempli wąskich (rys. 7). Zaznacza się dość silny wpływ prędkości v_0, szczególnie w zakresie od $0{,}005\frac{\text{mm}}{\text{s}}$ do $5\frac{\text{mm}}{\text{s}}$. Dalszy wzrost prędkości v_0 poza wartość $5\frac{\text{mm}}{\text{s}}$ nie ma już tak dużego wpływu na wielkość nacisków.

Porównując naciski graniczne wyznaczone teoretycznie i naciski wyznaczone doświadczalnie (na rys. 10 i 11 naniesiono dodatkowo linie teoretyczne $A_m B_m$, otrzymane przy założeniu warunku stanu granicznego Mohra), dochodzimy do następujących wniosków. Doświadczalne naciski graniczne marmuru tylko w małym zakresie $\frac{h}{a}\left(\frac{h}{a} \leqslant 30\right)$ i przy prędkościach $v_0 = 0{,}005$ i $0{,}5 \frac{\text{mm}}{\text{s}}$ odpowiadają w pewnym przybliżeniu naciskom teoretycznym (rys. 10). Przy narastających wartościach $\frac{h}{a}$ rozbieżność wyników doświadczalnych i obliczeniowych jest już znaczna, zwłaszcza przy większych prędkościach v_0. Gdy chodzi natomiast o wapień, wpływ wzrastającej prędkości v_0 nie odgrywa już tak znaczącej roli jak w wypadku marmuru (rys. 11).

Energia kruszenia obu skał jest największa przy stemplach szerokich, a prędkość odgrywa podobną rolę na wzrost tej energii, jak na wzrost nacisków, co jest widoczne na rys. 8. W znacznym zakresie wartości $\frac{h}{a}$ dla ustalonych prędkości v_0, energia pozostaje prawie niezmienna. Interesujące są wykresy energii w funkcji prędkości obciążania v_0 dla różnych $\frac{h}{a}$ (rys. 9). Otóż mają one maksimum przy prędkości $v_0 \approx 8 \frac{\text{mm}}{\text{s}}$ — marmur i przy $v_0 = 0{,}5 \frac{\text{mm}}{\text{s}}$ — wapień.

Pracę kończą rozważania o znaczeniu praktycznym.

Słowa kluczowe: mechanika kruszenia, stany graniczne, warunek Coulomba, zmodyfikowany warunek Coulomba, charakterystyki mechaniczne, naciski graniczne, energia kruszenia.

1. Introduction

A rock block compression realised by flat punches under conditions approximating two-dimensional strain state (Fig. 1a, b) is the important elementary process applied to model crushing processes in machines. This process and other model processes realised at small velocities were analysed on the background of limit state theories in previous works (Z a w a d a, 1976, 1995). The experimental verification of the theoretical solutions shows that for several domestic rocks there exists good compatibility of rock block crushing forces and crushing pattern. However, a question may be raised on possibilities to apply the obtained solutions for calculations of processes in which applied load velocities grow what causes the growth of inertia forces. In the limit state theory the effective methods for dynamic problems solutions have not been determined, even for the cases two-dimensional or axis — symmetrical deformation. The question is also essential in the context of rock behaviour under load velocity growth. Mostly the rocks show increasing resistance to deformation. However, there exists cases showing the opposite effect or insensitivity to velocity changes in a wide value range (M r ó z and M a j e w s k i, 1989), (K l e p a c z k o, 1983), (K i d y b i ń s k i et al., 1974).

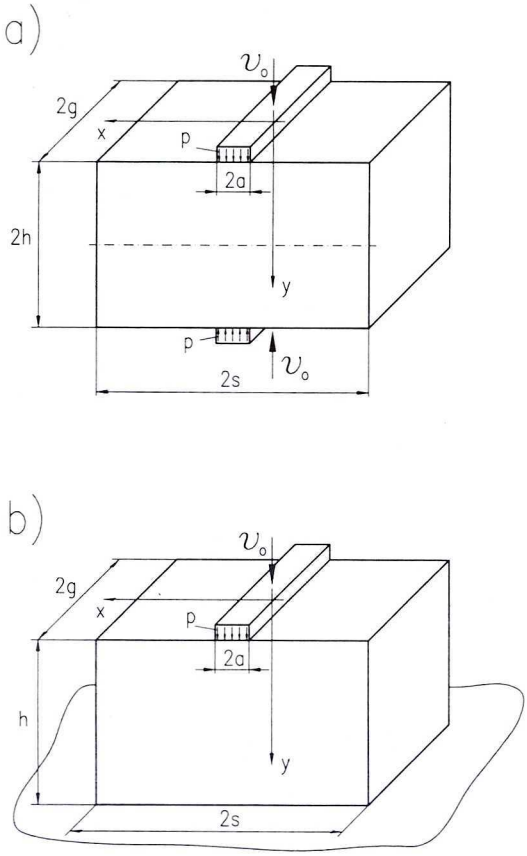

Fig. 1. The processes modelling real crushing process: a) compression of a block by flat co-axial punches; b) compression of a block by one punch

The other problem concerns the influence of load velocity on crushing forces, limit pressures, and fracture energy etc. There are no data on the theme in the specialised literature.

The paper is aimed at the answers to the above mentioned questions. It also determines the base to formulate certain preliminary conditions and direction for studies of crushing process optimisation.

2. The scheme of analysis of a block crushing by punches (Fig. 1)

The following assumptions would be taken (Z a w a d a, 1995), (S z c z e p i ń s k i, 1974):

- the process develops in two-dimensional strain state;
- the brittle body (rock) is homogeneous, isotropic and weightless medium;

- the rigid — ideally material plastic model describes the medium properties;
- the limit state condition (damage condition) is a function of stress state components σ_{ij}

$$F(\sigma_{ij}) = 0 \tag{1}$$

$$i = x, y \quad j = x, y;$$

- the physical law is the law associated with the limit state condition:

$$\varepsilon_{ij} = \lambda \cdot \frac{\partial F(\sigma_{ij})}{\partial \sigma_{ij}}, \tag{2}$$

where:

ε_{ij} — strain velocity tensor;
λ — positive scalar factor.

- compression stresses are considered positive (similarly dimensions decrease is positive).

It is additionally assumed that the deformation is located at the planes parallel to x, y co-ordinates plane. Axis y is directed vertically down. The stress and deformation velocity fields of the medium are defined if at its each point there are known the components of stress state $\sigma_x(x, y)$, $\sigma_y(x, y)$ and the components of deformation velocity: $v_x(x, y)$, $v_y(x, y)$. The stress component $\sigma_z(x, y)$ enclosed in the limits $\sigma_y \leqslant \sigma_z \leqslant \sigma_x$ does not have an effect accordingly to Mohr and Coulomb concept, on limit state condition. The velocity v_z is equal to zero. In order to define five components of stress state: $\sigma_x(x, y)$, $\sigma_y(x, y)$, $\tau_{xy}(x, y)$, $v_x(x, y)$, $v_y(x, y)$ we use:

1 — equilibrium equation $\frac{\partial \sigma_{ij}}{\partial x_j} = 0$
2 — limit state condition $F(\sigma_{ij}) = 0$ (1)
3 — physical law (2)

The equation system containing equilibrium conditions $\frac{\partial \sigma_{ij}}{\partial x_j} = 0$ and the limit state condition $F(\sigma_{ij}) = 0$, so called static equation system, enables to determine unknown stresses σ_x, σ_y, τ_{xy}. Kinematic equations system stemming from the relation $\dot{\varepsilon}_{ij} = \lambda \frac{\partial F(\sigma_{ij})}{\partial \sigma_{ij}}$ can be solved in the next step after the stresses are obtained. The solution of the system defines velocity field v_x, v_y.

The static and kinematic equations systems are solved by using the method of characteristics of quasi-linear partial differential equations (Zawada, 1995), (Szczepiński, 1974).

2.1. The linear Coulomb limit state condition

The solution of static equations lead to the following direction equations of two characteristic families α and β

$$\frac{dy}{dx} = \tan(\varphi + \varepsilon) \qquad \text{for } \alpha \text{ family}$$

$$\frac{dy}{dx} = \tan(\varphi - \varepsilon) \qquad \text{for } \beta \text{ family,} \tag{3}$$

where:

φ — stands for the angle which shows the direction of the maximum principal stress σ_1 in respect to x axis,

$\varepsilon = \frac{\pi}{4} - \frac{\varrho}{2}$ — defines the angle at which the maximum principal stress is rotated in relation to each characteristic.

The solution of the static equations lead to the following relations which are satisfied along the characteristics:

$$\begin{aligned} &d\sigma + 2\sigma \tan\varrho \, d\varphi = 0 \qquad \text{along } \alpha \text{ direction} \\ &d\sigma - 2\sigma \tan\varrho \, d\varphi = 0 \qquad \text{along } \beta \text{ direction} \end{aligned} \tag{4}$$

σ stands for auxiliary quality defined as an equivalent stress (Fig. 2a).

$$\sigma = \frac{\sigma_1 + \sigma_2}{2} + c \cdot \operatorname{ctg} \varrho \tag{5}$$

c — cohesion, ϱ — internal friction angle.

The characteristics equations for the velocities are obtained in the result of the solution of kinematic equations, for the family α and β respectively.

$$\begin{aligned} &\frac{dy}{dx} = \tan(\varphi + \varepsilon) \qquad dv_x + dv_y \operatorname{tg}(\varphi + \varepsilon) = 0 \\ &\frac{dy}{dx} = \tan(\varphi - \varepsilon) \qquad dv_x + dv_y \operatorname{tg}(\varphi - \varepsilon) = 0. \end{aligned} \tag{6}$$

The velocity characteristics coincide with stress characteristics. The stress characteristics net coincide with the velocity characteristics net.

2.2. Modified Coulomb condition

The main negative feature of the Coulomb condition is, in general, non realistic description of rock properties. One of the ways to correct this state for the tension

zone may be introduced by cutting linear envelopes with an arc of a circle with the radius R_z (Fig. 2a):

$$R_z = \frac{1}{2}S_c - H\frac{\sin\varrho}{1-\sin\varrho}, \tag{7}$$

where:

S_c — uniaxial strength;

H — isotropic tension strength identified, in this condition, with uniaxial tension strength S_{rz}.

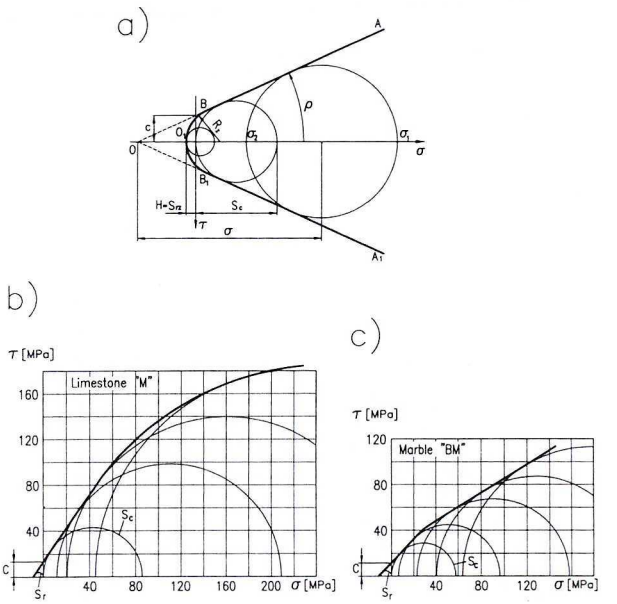

Fig. 2. Theoretical and real limit state conditions: a) linear Coulomb condition — line OA and OA_1, modified Coulomb condition — line O_1BA and $O_1B_1A_1$; b), c) real envelopes of limit state for marble "BM" and limestone "M"

If the stresses in the limit zone represent Mohr circles of R radius greater than R_z the linear Coulomb condition can be applied, so the equation (3), (4), (6) are valid. In the case when the circles $R \leqslant R_z$ represent the limit state it means that internal friction angle ϱ reaches the value $\varrho = \frac{\pi}{2}$. Than we have one family straight line characteristics represented by direction equation:

$$\frac{dy}{dx} = \tan\varphi \tag{8}$$

and by the following relation for velocities along this family:

$$dv_x + dv_y \operatorname{tg}\varphi = 0. \tag{9}$$

2.3. The stress and velocity characteristics net (the problem shown at Fig. 1b) — Coulomb condition

So called stress field prediction method is used (Szczepiński, 1978, p. 69). It is assumed that pressure developed under the punch is homogeneous thus the homogeneous stress state occurs in the triangle ABC (Fig. 3). In the curvilinear triangles ACE and BCD we have characteristic problem with singular points A and B, while there appears characteristic problem in quadrangle $ECDF$. Symmetrically developed at both sides of the block the nets get in contact at central point F of symmetry axis. The stresses represented as a function of unknown pressures p can be found at each knot point of the characteristic net. The value of these pressures corresponding to the block height h and punch width $2a$ ratio are determined by integral condition of resultant horizontal stress σ_x loss at vertical symmetry axis y.

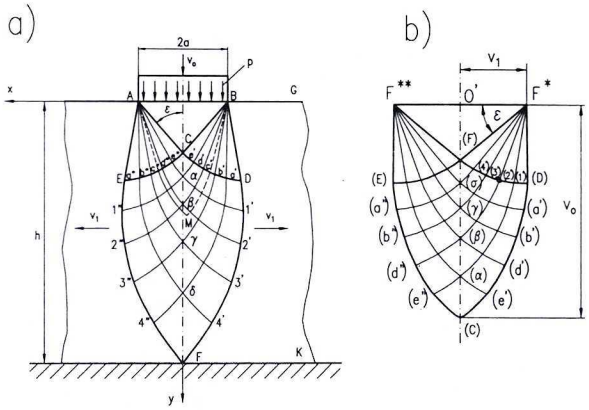

Fig. 3. The solution of the block crushing process developed by a punch, Coulomb condition: a) characteristics net, b) hodograph

The displacement velocity of points of limit zone $ABDFE$ are found by using relations (6) or by simpler method by drawing velocity field — hodograph (Fig. 3b). Individual points of hodograph net describe respective velocities of displacement of limit zone points. For example, vector which connects pole O' and point (D), that is vector $O'(D)$ defines velocity of displacement of point D (Fig. 3a) belonging to the limit zone. Vector $O'F^*$ describes displacement velocity of the zone $BFGK$ which is in the rigid state (undeformed).

2.4. Characteristics net — modified Coulomb condition

The characteristics net is shown at Fig. 4. The zone bounded under the punch is defined by characteristic AEF representing the family α and characteristic BDF representing the family β (3). The stress state in this zone is found by solving basic

boundary problem with relations (4) used which were derived for linear Coulomb condition ($\varrho = \text{const}$). There appears below the area $AEFDB$ one characteristic FG (8) where the tension stress $\sigma_2 = S_{rz}$ and compression stresses σ_1 operate. The two stresses are represented by Mohr circle with radius R_z (Fig. 2a). The point F is the singular point where internal friction angle changes the value within the limits $\varrho = \text{const}$ to $\varrho = \frac{\pi}{2}$.

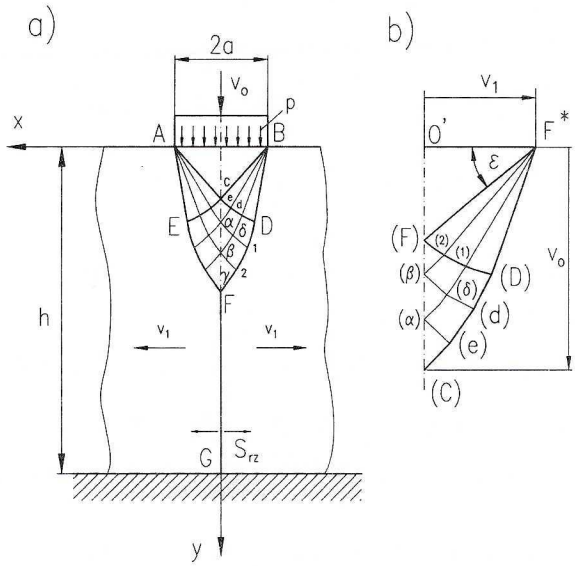

Fig. 4. The solution of the block crushing process developed by a punch, modified Coulomb condition: a) characteristics net, b) hodograph

3. Experimental studies

The experimental studies made within the framework of *CPBP* 03.07 [1] project (Z a w a d a et al., 1989), dealt with loading samples according to the scheme given at Fig. 1b. Two kinds of domestic rocks were tested marble [2] from region of Stronie Śl. and limestone [3] taken at Kielce region. Their real envelopes of limit state are shown at Fig. 2b, c (Z a w a d a, 1998, page 85).

---

[1] Studies of foundations of minerals' enrichment.

[2] Middle grain marble (Biała Marianna "BM") is a very hard rock with small absorbability, small strength and high grindability — according to PN-62/B-01080 standard.

[3] Thick limestone (Morawica "M") is a very hard rock with small absorbability and moderate strength and grindability according to PN-62/B-01080 standard.

3.1. Strength properties characteristic of tested rocks

The limit state condition of "BM" marble can be approximated by linear Coulomb condition $|\tau| = \sigma \operatorname{tg} \varrho + c$

$$|\tau| = \sigma \operatorname{tg} 31^\circ + 20 \quad [\text{MPa}] \tag{10}$$

or more precisely by modified Coulomb condition with radius $R_z = 26.3$ MPa, and uniaxial tension strength $S_{rz} = -8$ MPa (the meaning of R_z and S_{rz} is described at Fig. 2a). The limestone "M" shows the following values

$$|\tau| = \sigma \operatorname{tg} 54^\circ + 20 \quad [\text{MPa}] \tag{11}$$

$$R_z = 10\,\text{MPa} \qquad S_{rz} = -12\,\text{MPa}.$$

3.2. The data on samples, punches, load velocity and tests technique

The samples with dimensions: height $h = 30$ mm, width $2s = 50$ mm, thickness $2g = 10$ mm were cut out of bigger blocks by circular saw. The widht of pressing punches was $2a = 0.5$; 1.0; 2.2; 4.0; 10[mm]. Thus, the value of the ratio $\frac{h}{a}$ changed between the limits 6,0 to 120. The velocity v_0 of the punch displacement reached the values: 0.005; 0.5; 5.0; $50 \frac{\text{mm}}{\text{s}}$ for the marble and $v_0 = 0.005$; 0.5; 5; $100 \frac{\text{mm}}{\text{s}}$ for the limestone. The tests were repeated several times for certain values of $\frac{h}{a}$ and v_0.

The experiments were made at "Instron" (model 1251) testing machine equipped with computer control and recording systems. The sample was fastened to polished plate of machine lower cross-bar. The punch was secured in special cap-and-ball joint holder. The hydraulic servo-motor displacement served as control parameter. The linear increase of this displacement developed in a certain time resulted in achieving programmed velocity v_0. The changes of the punch loading force and its displacement were recorded.

3.3. The test results

The most important test results would be given in tables 1 and 2 as well as in graphical form. The table 1 contains marble "BM" data and the table 2 limestone "M" data. These data describe maximum values of forces (thus limit forces) appearing at loading processes developed for different punch widths $2a$, different load velocities v_0 as well as the energy of fracture (crush) process.

TABLE 1

Marble "BM". Maximum values of forces (limit forces) and energy of fracture (crush) for different punch widths, $2a$, and load velocities, v_0, (medium values)

$2a$ [mm]	$V_0\left[\frac{\text{mm}}{\text{s}}\right]$			
	0.005	0.5	5.0	50.0
0.5	F_{max} [kN] 1.938	2.273	5.938	6.75
	E_K [J] 0.138	0.162	1.019	0.648
0.96	F_{max} 2.991	6.369	8.350	8.60
	E_K 0.162	0.328	0.890	0.739
2.2	F_{max} 4.066	5.681	11.525	12.612
	E_K 0.171	0.447	1.402	1.35
4.0	F_{max} 6.872	7.20	17.05	17.587
	E_K 0.391	0.594	2.127	1.891
10.0	F_{max} 8.338	20.338	31.075	35.775
	E_K 0.788	2.765	4.965	5.495

TABLE 2

Limestone "M". Maximum values of forces (limit forces) and energy of fracture (crush) for different punch widths, $2a$, and load velocities, v_0, (medium values)

$2a$ [mm]	$V_0\left[\frac{\text{mm}}{\text{s}}\right]$			
	0.005	0.5	5.0	100
0.5	F_{max} [kN] 4.95	6.57	7.1	6.747
	E_K [J] 0.389	0.523	0.674	0.625
0.96	F_{max} 4.48	9.75	11.0	9.04
	E_K 0.267	1.128	1.198	0.808
2.2	F_{max} 7.67	17.75	19.2	15.75
	E_K 1.087	2.461	2.658	1.873
4.0	F_{max} 22.7	24.23	29.8	25.6
	E_K 2.58	4.0	4.287	3.92
10.0	F_{max} 28.66	44.0	49.7	42.4
	E_K 4.085	12.41	10.61	7.339

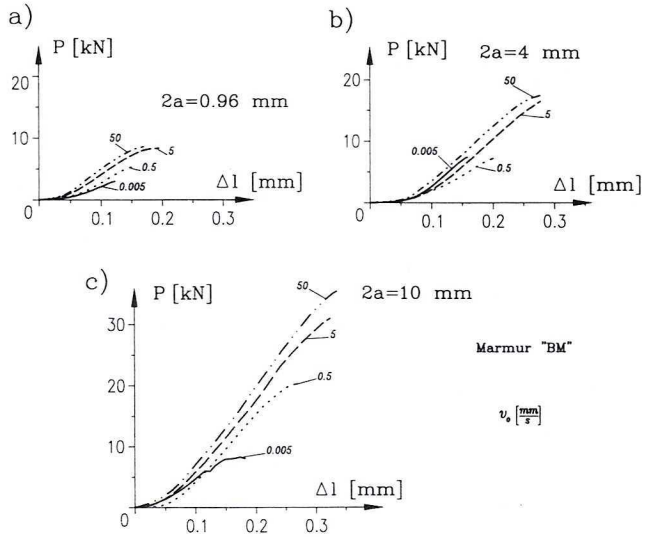

Fig. 5. Mechanical characteristics (force — displacement) of marble "BM" corresponding to various velocities v_0

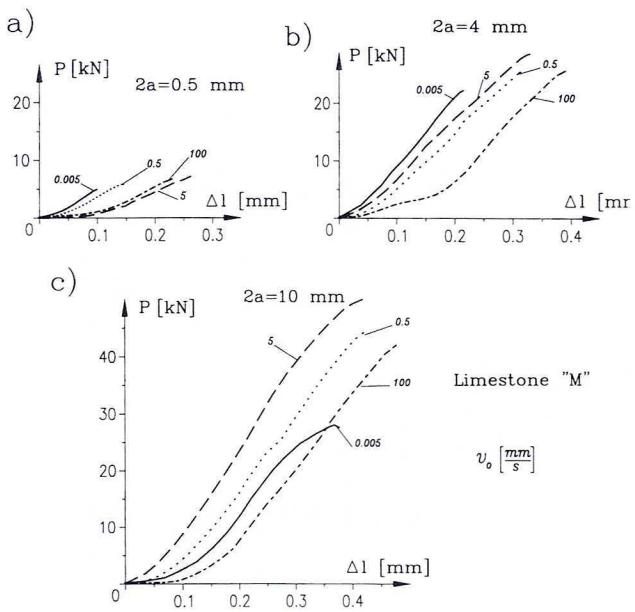

Fig. 6. Mechanical characteristics of limestone "M" corresponding to various velocities v_0

The energy dissipated in a certain process corresponds to the area under force versus displacement graph. The maximum limit value of force co-ordinate is assumed as the graph last point. The energy value was obtained directly on the base of computer files.

The presented graphs correspond to:

• examples of mechanical characteristics that is dependence of load force P on punch displacement Δl; for the marble "BM" (Fig. 5) the presented characteristics were obtained when narrow ($2a = 0.96$ mm), medium ($2a = 4$ mm) and wide ($2a = 10$ mm) punches were used together with velocity $v_0 = 0.005;\ 0.5;\ 5.0;\ 50 \frac{\text{mm}}{\text{s}}$; similarly for limestone "M" (Fig. 6) the presented characteristics correspond to narrow ($2a = 0.5$), medium ($2a = 4$ mm) and wide ($2a = 10$ mm) punches displaced at velocity $v_0 = 0.005;\ 0.5;\ 5.0;\ 100 \frac{\text{mm}}{\text{s}}$;

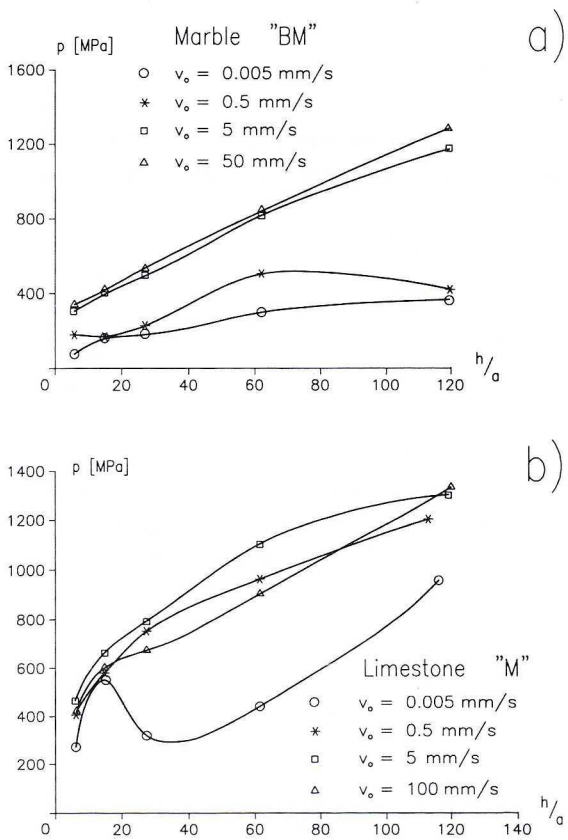

Fig. 7. Limit pressures p as function of h/a for various v_0: a) marble "BM", b) limestone "M"

- limit pressures p as function of $\frac{h}{a}$ ratio at different velocities v_0; these pressures were calculated by relation $p = \frac{P}{2a \cdot 2g}$, where P stands for maximum force providing for sample damage; experimental points represent the average of several tests (Fig. 7);
- fracture (crush) energy E_K as a function of $\frac{h}{a}$ ratio for different v_0 (Fig. 8);
- fracture energy E_K as a function of velocity v_0 for different values of $\frac{h}{a}$ (Fig. 9).

4. The test results analysis

4.1. Mechanical characteristics $P-\Delta l$ (Fig. 5 and 6)

The marble "BM" reacts in the similar way as the most rocks do at increasing velocities of load application what means that the deformation resistance of the medium grows respectively to punch displacement velocity. It can be noted at Fig. 5 that the maximum limit forces correspond to maximum velocities of loading and, in general, correspond to maximum displacement. The characteristics graphs that suit punches $2a = 4$ mm and $2a = 10$ mm are deformed to some extend at velocity $v_0 = 0.005 \frac{\text{mm}}{\text{s}}$ and $v_0 = 0.5 \frac{\text{mm}}{\text{s}}$.

It turns out much more difficult to interpret mechanical characteristics of limestone "M". There appears a strange effect which distinctly visible for punches $2a = 10$ mm and $2a = 4$ mm expresses decrease of resistance of rock (and value of limit force) at maximum velocity of loading $v_0 = 100 \frac{\text{mm}}{\text{s}}$. The curves $P = f(\Delta l)$ corresponding to other velocities v_0 also differ from typical shapes obtained for rocks. The reason of such a dissimilarity of "M" limestone behaviour has not been cleared. The additional tests are recommended in order to check the experimental results presented in the paper. The deformation mechanism related to structure changes of the rock should be additionally studied.

4.2. Limit loads (pressures)

Limit presures p, what is also predicted by limit state theory, increase for growing of h/a, thus come to maximum for narrow punches (Fig. 7). There is observed the strong influence of velocity v_0, in particular in the range of 0,005 mm/s (very slow quasi-static loading) to do 5 mm/s. Further increase of velocity v_0 beyond the value 5 mm/s does not have such a significant influence on magnitude of pressures. For

marble $\left(\text{at fixed value } \frac{h}{a}\right)$ the increase of velocity v_0 causes simultaneous increase of p. In the case of limestone we do not observe such a regularity (Fig. 7b). The maximum limit loads appear, for example, at $v_0 = 5$ mm/s and are greater than at $v_0 = 100$ mm/s.

Now we proceed to comparison of theoretical and experimental results. At Fig. 10 and 11 there are marked these solutions for both rocks. The lines ABC represent theoretical curves obtained for linear Coulomb condition. The lines $AZ_{m1}C$ i $AZ_{m2}C$ represent theoretical curves of marble (Fig. 10) obtained for modified condition with $k = S_c/S_{rz} = 5$ and 10 respectively. The symbols S_c stands for uniaxial compression strength, and S_{rz} stands for uniaxial tension strength (Fig. 2a). The test results indicate that for marble "BM" value of the factor $k = S_c/S_{rz}$ lies between the limits 5–10. Similarly, at Fig. 11 the lines AB and AZ_m denote theoretical lines of limestone "M" for Coulomb condition and modified condition with $k = 15$ assumed. Additionally, at both figures theoretical lines A_mB_m, were drawn. The lines match Mohr limit condition formulated as a relation $\left(\frac{\tau}{c}\right)^n - \frac{\sigma}{H} - 1 = 0$, where symbols c and H denote already mentioned material constants: cohesion and isotropic tension strength while τ and σ denote tangent and normal stresses operating at slip planes. The experimental factor n is constrained by the limits $1 \leqslant n \leqslant 2$. The Mohr condition as well as the theory of stress state and velocity of medium displacement developed for this condition were carefully discussed by J. Zawada in monograph of 1995.

The limit pressures of "BM" marble, at certain approximation, match theoretical pressure predictions only in a small range of $\frac{h}{a}$ $\left(\frac{h}{a} \leqslant 30\right)$ and for velocities $v_0 = 0.005$ and $0.5\left[\frac{\text{mm}}{\text{s}}\right]$. The experimental and theoretical results discrepancies come to significant values for increasing values $\frac{h}{a}$ and, in particular, for higher velocities v_0. In the case of limestone "M" the influence of increasing velocity is not so significant as it was observed for marble "BM". It is interesting although it has not been cleared yet, that good compatibility of experimental and theoretical results can be noted at significant velocity $v_0 = 100\frac{\text{mm}}{\text{s}}$, especially for high values $\frac{h}{a}$. The introduced additional theoretical line A_mB_m (Mohr condition) describes, in relatively good way, the relation of pressures $\frac{p}{c}$ for the smallest velocity $v_0 = 0.005\frac{\text{mm}}{\text{s}}$.

What conclusions come out of this preliminary experimental verification? The limit pressures obtained in the experiments for "BM" marble, in general, are not

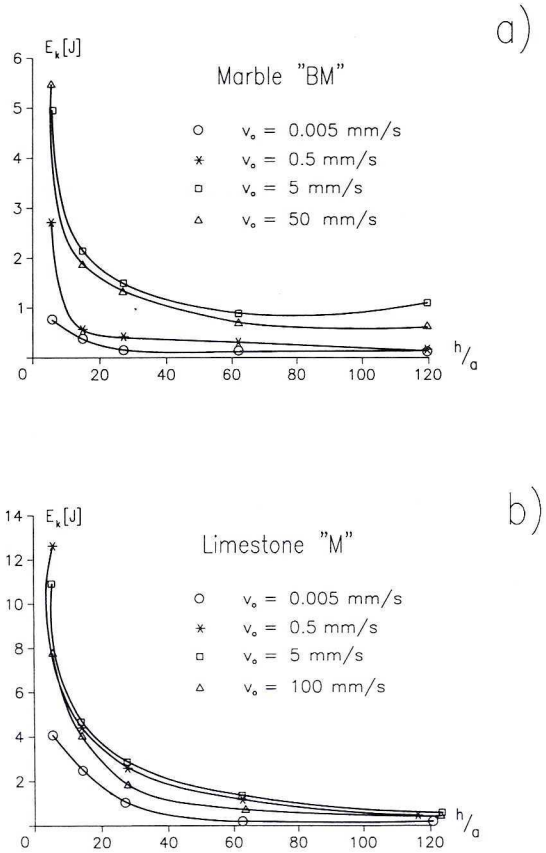

Fig. 8. Energy of fracture (crushing) as a function of h/a for various v_0: a) marble "BM", b) limestone "M"

close to theoretical values either at small $\left(v_0 = 0.005\frac{\text{mm}}{\text{s}}\right)$ or at significant $\left(v_0 = 50\frac{\text{mm}}{\text{s}}\right)$ velocity values. The reason of these discrepancies may likely come from the applied for calculations, limit curve which was defined some time ago for the rock of different ledge. Another reason may arise from too small number of tests (4; 5 samples) repeated for the same parameters (given value $\frac{h}{a}$ and velocity v_0). The experimental pressures for limestone "M" are closer to theoretical results than those obtained for marble "BM", especially at increasing values $\frac{h}{a}$. The two rocks, undoubtedly, require wide and detailed experimental studies, as the presented results contain significant discrepancies.

4.3. Crushing energy

The crushing energy of both rocks gains the maximum value for the wide punches $\left(\text{small values } \frac{h}{a}\right)$. The influence of velocity on the crushing energy is similar as it can be observed in the case of pressure increase what is shown at Fig. 8. In the wide scope of $\frac{h}{a}$ values, for settled velocities v_0 the energy remains almost constant. For the increasing $\frac{h}{a}$ that is for decreasing punch widths the differences of damage energy are insignificant at various velocities v_0 $\left(\text{for marble "BM" } v_0 = 5;\ 50\ \left[\frac{\text{mm}}{\text{s}}\right];\right.$ $\left.\text{for limestone "M" } v_0 = 0.5;\ 5,\ 100\frac{\text{mm}}{\text{s}}\right)$. This is an important observation.

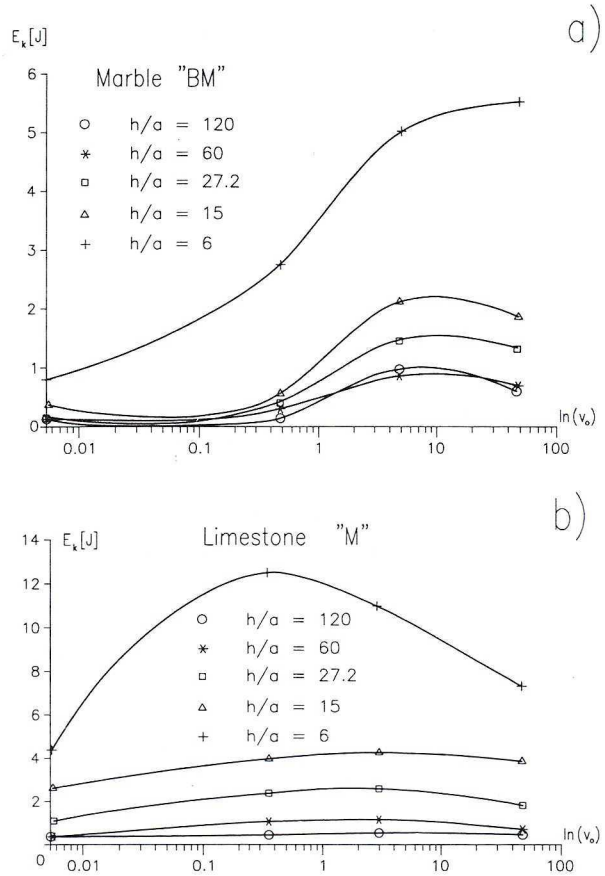

Fig. 9. Energy of fracture (crushing) as a function of velocity v_0 for various h/a: a) marble "BM", b) limestone "M"

The graph of energy against load velocity v_0 obtained for various $\frac{h}{a}$ (Fig. 9) bring some interest. And so, the energy maximum value corresponds to velocity $v_0 \approx 8 \frac{\text{mm}}{\text{s}}$ for marble "BM" and $v_0 = 0{,}5 \frac{\text{mm}}{\text{s}}$ for limestone "M". The energy function rapidly grows to reach a peak value and than rapidly falls for $2a = 10$ mm load punch applied. The energy function for marble (the same punch) expresses the similar character. This function, however, reveals slow progress for different punches what indicates little influence of increasing velocities on its values.

It is worth mentioning that limit state theory based on rigid-plastic model (of body) eliminates the possibility to calculate damage energy, However, the estimation of damage power that is external limit load power, is possible. The virtual power rule formulates that power of energy D dissipated inside a body of V volume equals to power developed by external loads:

$$\dot{D} = \int_V \sigma_{ij} \cdot \dot{\varepsilon}_{ij} \cdot dV. \tag{12}$$

Having determined stress and velocity fields over the limit area the internal dissipation power can be calculated. Thus, the comparison of theoretical to real crushing energy could also be made.

5. Concluding remarks

The applied load velocities v_0 belonged to rather wide range starting at small values and coming to reasonable values. The strain velocity $\dot{\varepsilon}$ which is one of the basic qualities in the theory of limit state depends on load velocity v_0. In the presented experiments strain velocity $\dot{\varepsilon}$ reached values of $1.6 \cdot 10^{-4} - 1.7$ [1/s] for marble and $1.6 \cdot 10^{-3} - 4.28$ [1/s] for limestone.

So, the loads might have been treated as quasi-static for which $\dot{\varepsilon} < 10^{-2}$ [1/s] is assumed, or as loads of intermediate character with $\dot{\varepsilon} = 10^{-2} - 10^{2}$[1/s].

The question on practical application of the presented studies occurs (apart from the fact that the experimental and theoretical results shown significant discrepancies). The examples of the answer deal with estimation of limit loads developed in crushing chambers of jaw crushes, calculations of model processes for machines of this group, calculations of crushing energy etc.

Let us analyse, as in the following example, the method of calculating limit loads in crushing chamber of double toggle crusher R 40.15 (produced by "Makrum" factory) disintegrating limestone "M". The maximum linear velocity of moving jaw of this crusher did not exceed the value $v_0 = 0.25 \left[\frac{\text{mm}}{\text{s}}\right]$, and maximum acceleration $a = 10 \frac{\text{mm}}{\text{s}^2}$.

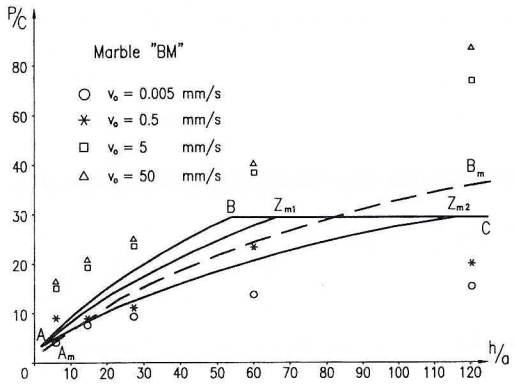

Fig. 10. Marble "BM" — verification of theoretical solutions

The material strain velocity $\dot{\varepsilon}$ for this machine satisfied the condition $\dot{\varepsilon} < 5\,[1/s]$. The values $\frac{h}{a}$ (that is height of disintegrated blocks to notches width of working plates so called "jaws") belonged to the range 30–80. If the line AB (Fig. 11) relates to unique solution of the problem then let the line A_gB_g to show so called upper bound solution of the complete solution. The upper bound solution can be obtained in the complete form by using limit analysis methods applied, for example, in rock and soil mechanics (I z b i c k i and M r ó z, 1976). It can be suggested, however, for the purpose of engineering calculations that a certain simplified method should be used. Accordingly, we assume that the upper solution coincides with maximum limit loads which may appear in the experiments series containing several or dozen samples. In other words, we are interested in upper deviation from average loads.

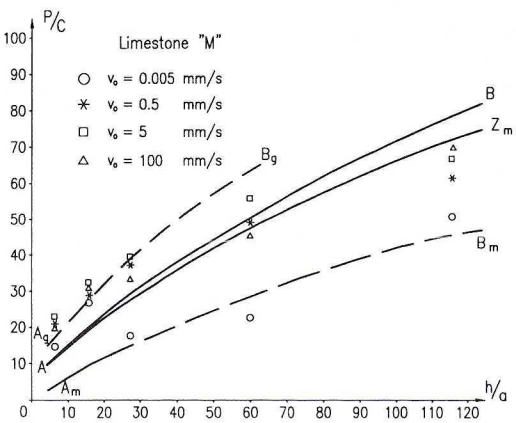

Fig. 11. Limestone "M" — verification of theoretical solutions

In the case of rocks these upper deviations (as well as lower deviation that is the results scatter) express significant values which approach or even exceed 30% of the average value (Zawada, 1995, p. 105). The ordinates of line A_gB_g, in accordance to this assumption, would denote 1.3 of the ordinates values of line AB. Having known the run of line A_gB_g we estimate upper values of limit pressures for the given $\frac{h}{a}$ range. The presented approach, although simplified seems to be justified for the analysed crusher.

At the end it should be mentioned that studies of crushing processes developed under dynamic loads, when $\dot{\varepsilon} > 10^2$ 1/s, can be carried out by means of Hopkins rods technique. Some preliminary results of such experiments are presented in reports (Zawada et al., 1986, 87, 88).

REFERENCES

Izbicki R. J., Mróz Z., 1976. Limit analysis methods for soils and rocks mechanics. PWN, Warszawa – Poznań.

Kibybiński A., Smołka, J., Bałazy I., 1974. Specification of basic mechanical properties of heavy rocks. Komunikat nr 606. Główny Instytut Górnictwa, Katowice.

Klepaczko, J., 1983. On the rate sensivity of coal. Engng. Trans., 31, 3, 341 – 360.

Mróz Z., Majewski E., 1989. Dynamic model of damage of coal and of some rocks for specifications of rock burst mechanisms. Arch. of Min. Sci., 34, 1, 65 – 95.

Szczepiński W., 1974. Limit states and kinematics of grain media. PWN, Warszawa.

Szczepiński W., 1978. Mechanics of plastic flow. PWN, Warszawa.

Zawada J., 1976. Analysis of rock block compression by flat punches. Rozpr. Inż., 24, 3, 579 – 599.

Zawada J., Supel J., Dietrich, L., 1986, 1987, 1988. Studies on rocks under dynamic load conditions. Sprawozdania z prac badawczych. Instytut Maszyn Roboczych Ciężkich, Politechnika Warszawska, Warszawa.

Zawada J., Supel J., Dietrich L., 1989. Analysis of influence of the system: tool — brittle medium on crushing process. Instytut Maszyn Roboczych Ciężkich, Politechnika Warszawska, Warszawa.

Zawada J., 1995. Limit loads and fracture of rocks (in model crushing processes). Wydawnictwo Naukowe PWN, Warszawa.

Zawada J., 1998. Introduction to mechanics of crushing processes. Wydawnictwo: Instytut Technologii Eksploatacji, Radom.

REVIEW BY: PROF. DR HAB. INŻ. JERZY GUSTKIEWICZ, KRAKÓW

Received: 23 November 1998.